Journal of Geochemical Exploration 108 (2011) 88–98

Contents lists available at ScienceDirect

Journal of Geochemical Exploration

journal homepage: www.elsevier.com/locate/jgeoexp

Chemical and isotopic composition of diagenetic carbonate cements and its relation to hydrocarbon accumulation in the Heletz-Kokhav oil field (Israel)

Ran Calvo [a,b,*], Avner Ayalon [a], Amos Bein [a,1], Eytan Sass [b]

[a] Geological Survey of Israel, 30 Malkhei Israel Street, Jerusalem 95501, Israel
[b] Institute of Earth Sciences, The Hebrew University of Jerusalem, Jerusalem 91904, Israel

ARTICLE INFO

Article history:
Received 3 March 2010
Accepted 14 October 2010
Available online 26 October 2010

Keywords:
Hydrocarbon accumulation
Oxygen and carbon stable isotopes
Carbonate chemistry
Diagenesis
Heletz Formation

ABSTRACT

Israel's recent offshore gas discovery and possible onshore oil discoveries put Israel as an energy independent country. Up to now, the Heletz-Kokhav oil field is the largest oil finding in Israel. The main reservoir units in this oil field contain sandstone and shale layers intercalated with limestone and dolostone of the Lower Cretaceous Heletz Formation, found at an average depth of about 1600 m below surface on the Israeli coastal plain. The chemical composition and isotopic values ($\delta^{13}C$ and $\delta^{18}O$) of the carbonate cement minerals along with the paragenetic sequence have been used to identify the changes in the pore-water composition during the diagenesis of the clastic rocks.

The diagenetic carbonate phases in the clastic units include early low-Mg calcite ($\delta^{18}O_{Calcite}$ of −3.53 and −3.46‰ VPDB; $\delta^{13}C_{Calcite}$ of -2.53 and + 1.15‰ VPDB) and siderite ($\delta^{18}O_{Siderite}$ of −4.28 and + 1.45‰; $\delta^{13}C_{Siderite}$ of −4.22 and −2.65‰). Ankerite, the dominant authigenic phase in the Heletz Formation (average composition of $Ca_{1.09}Mg_{0.62}Fe_{0.28}Mn_{0.013}(CO_3)_2$ with $\delta^{18}O_{Ankerite}$ of −4.73 to + 0.52 ‰ and $\delta^{13}C_{Ankerite}$ of −11.92 to + 0.04‰), and low-Mg poikilotopic calcite ($\delta^{18}O_{Calcite}$ of −8.77 to −2.84‰; $\delta^{13}C_{Calcite}$ of −9.45 to −1.60‰) were formed later in the diagenetic history. Fracture-related diagenesis of ankerite, dolomite, and high-Mg calcite ($\delta^{18}O_{Calcite}$ of -6.86 to -1.66‰; $\delta^{13}C_{Calcite}$ of -12.94 to + 1.74‰) is found in the dolostone rocks of Kokhav Dolomite Member.

Petrographic interpretation, the iron content in the ankerite, and the $\delta^{13}C$ values indicate that the formation of the ankerite took place during the migration and accumulation of hydrocarbons in the Heletz trap.

Based on the $\delta^{18}O$ values, we suggest that early in the burial history shallow diagenesis (calcite, siderite) occurred in the presence of fresh water within different levels of oxic to redox microenvironments. As burial proceeded, the $\delta^{18}O$ values of the pore-water increased due to water/rock interaction. Ankerite and calcite cement were deposited from this ^{18}O-enriched water at or near maximum burial temperatures (~ 60 °C). Fracture-related diagenesis of vein filling minerals (ankerite, dolomite and calcite) took place very late in the diagenetic history, probably during the Messinian desiccation event of the Mediterranean Sea (Upper Miocene) from the Mavqi'im seawater penetrating into the subsurface of the coastal plain of Israel. The reconstructed burial and diagenetic history attest to a large-scale pore-water movement in this sedimentary basin, even down to several thousand meters below surface.

1. Introduction

Shallow, early diagenetic minerals in continental clastic sediments usually precipitate from meteoric-derived pore water, but mixing with marine water occurs in near-shore and coastal sediments (Morad et al., 1994). During burial diagenesis, mixing of these shallow diagenetic waters with subsurface brines occurs along with water–rock interactions, and hence profound changes in the formation water chemistry are common (Longstaffe, 2000). These geochemical changes of pore water, combined with elevated temperatures and pressures, are expected to be reflected in the geochemical composition of the diagenetic minerals in the host sediments.

The Lower Cretaceous Heletz Formation was penetrated by many boreholes, mainly in the Heletz-Kokhav oil field, located in the southern coastal plain of Israel (Fig. 1). In this area, 370 m of intercalated sandstone, shale, limestone and dolostone is found at an average depth of about 1600 m. The main diagenetic phases in the Heletz Formation are carbonate minerals (calcite, ankerite, dolomite and siderite), a few silicate minerals (quartz, K-feldspar, kaolinite, illite, smectite, and I/S) and pyrite (Shenhav, 1971; Calvo, 1992; Calvo et al., 1993, 1995).

* Corresponding author. Geological Survey of Israel, 30 Malkhei Israel Street, Jerusalem 95501, Israel. Tel.: +972 2 5314299; fax: +972 2 5380688.
E-mail address: rani.calvo@gsi.gov.il (R. Calvo).
[1] Current address: RPD-Geohyd Consultants, 21 Hamagalit Street, Jerusalem 97277, Israel.

0375-6742/$ – see front matter © 2010 Elsevier B.V. All rights reserved.
doi:10.1016/j.gexplo.2010.10.008

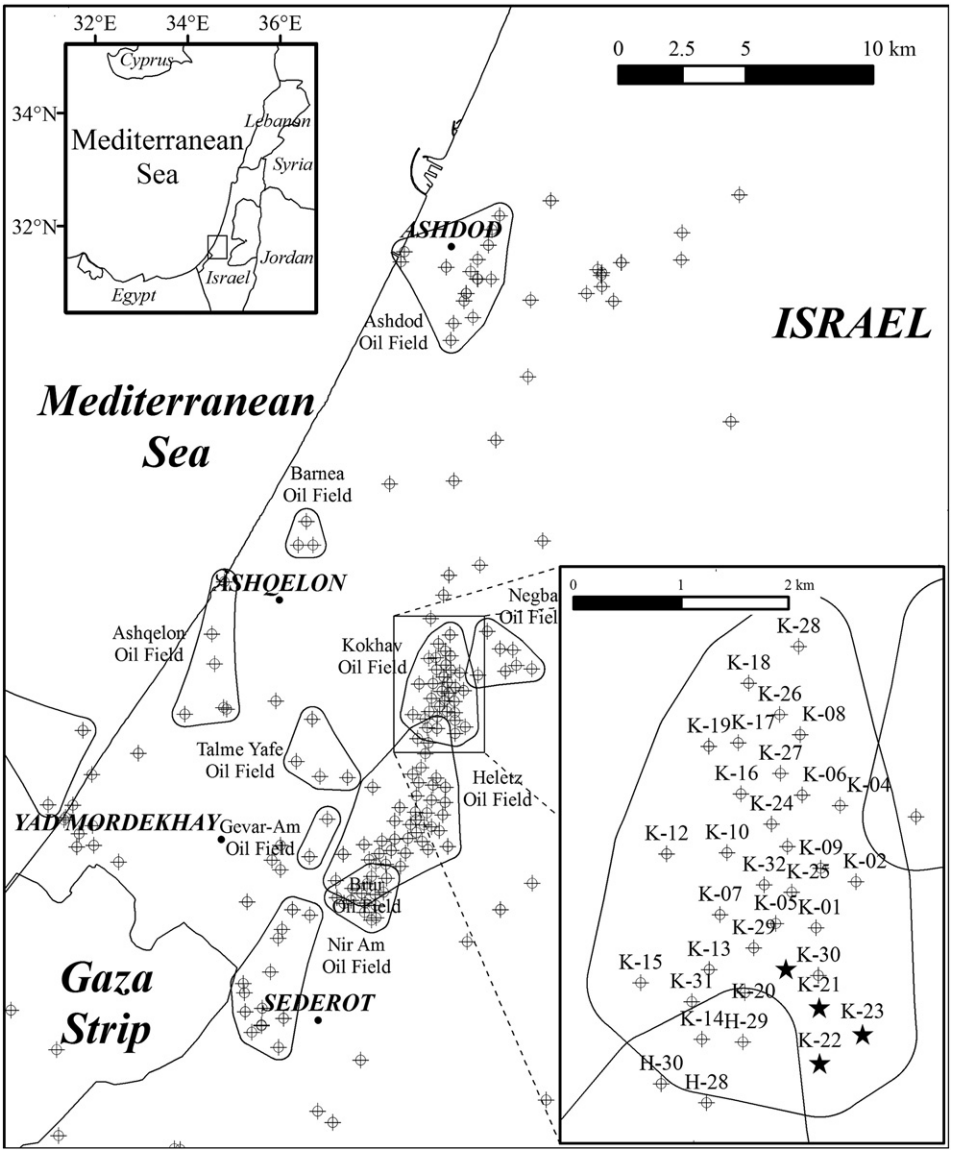

Fig. 1. Location map of the study area and the oil fields in southern Israel (after Shenhav, 1971, and Bein and Sofer, 1987). The Nir-Am, Brur, Heletz, Kokhav, and Negba oil fields are located along the axis of the Heletz anticline structure.

The aim of the current study was to conduct a chemical and stable isotope study of all diagenetic carbonate occurrences and to establish a paleohydrological reconstruction of the evolution of large-scale pore-water movement in the sedimentary basin of the coastal plain of Israel, which in now-days extensively studied and drilled for oil and gas exploration.

2. Geological setting

The Lower Cretaceous (Valanginian to Barremian) Heletz Formation was deposited in partly near-shore-to-coastal and partly pelagic environments (Picard, 1959; Grader, 1959; Grader et al., 1960; Cohen, 1971) and thus consists of a series of shale and sandstone layers intercalated with limestone and dolostone. The Heletz-Kokhav oil field area was located at the shelf break (Bein and Gvirtzman, 1977), which marked the margins of the Arabian Shield. On the eastern side, platform sediments were deposited over a gently inclined Jurassic erosion surface, while on the basinward side a shaly facies was deposited, leading to the interfingering of the clastic units of the Heletz Formation with the shales of the Gevar-Am Formation (Aharoni, 1964).

The sandstones are mainly quartz-arenite and subarkose with some arkose, and range from tuffaceous sandstone to ankeritic sandstone and siltstone (Shenhav, 1971). Diagenetic phases include early burial calcite and siderite, followed, after rapid burial (~50 m/Ma), by quartz and K-feldspar overgrowth (some 90 Ma ago, K-Ar dating). Dolomite, ankerite, calcite, pyrite and clays (kaolinite, illite, I/S, and smectite) were formed later in the diagenetic history (Fig. 2), till 76 Ma ago (K-Ar dating of the illite). Fracture-related diagenesis of pyrite, ankerite, dolomite, and calcite is found in the dolostone rocks of the Kokhav Dolomite Member (Calvo, 1992; Calvo et al., 1993, 1995).

The interfingering of the sandstones (Middle Sand and Lower Sand members) and shales (Rewaha Shale and Nehora Shale members; Fig. 3) created a natural stratigraphic oil trap (Cohen, 1971; Bein and Sofer, 1987; Gilboa et al., 1990). During the Upper Cretaceous to Middle Eocene a symmetrical anticline was formed in the Heletz-Kokhav area as part of the tectonic activity of the Syrian Arc folding system. The Heletz anticline is aligned in a northeast to southwest direction, forming the structural trap of the Heletz-Kokhav oil field. The sands and dolomites in the formation exhibit good reservoir characteristics for oil. The main pay zones in the Heletz-Kokhav oil

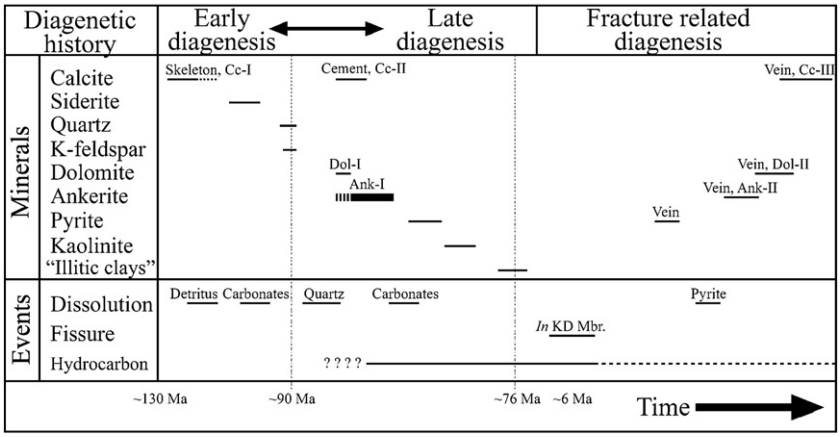

Fig. 2. The paragenetic sequence of the authigenic minerals and events in the Heletz Formation.

field are (from bottom to top) the sandy layers KAS and KBS of the Kokhav sands unite (Lower Sand Member) (Fig. 3), the dolomite layer KD of the Kokhav Dolomite Member, the sandy layers HKS, HWS, HAS and HZS of the Heletz sands unit (Middle Sand Member), and the LC11 limestone layer (Cohen, 1971).

Bein and Sofer (1987) stated that the hydrocarbons in the Heletz-Kokhav oil field were derived from the Jurassic carbonate source rocks, buried to the west of the oil field area at a depth of over 4500 m. Organic maturation considerations suggest that migration started only after Miocene times (Bein and Sofer, 1987). Petrographic

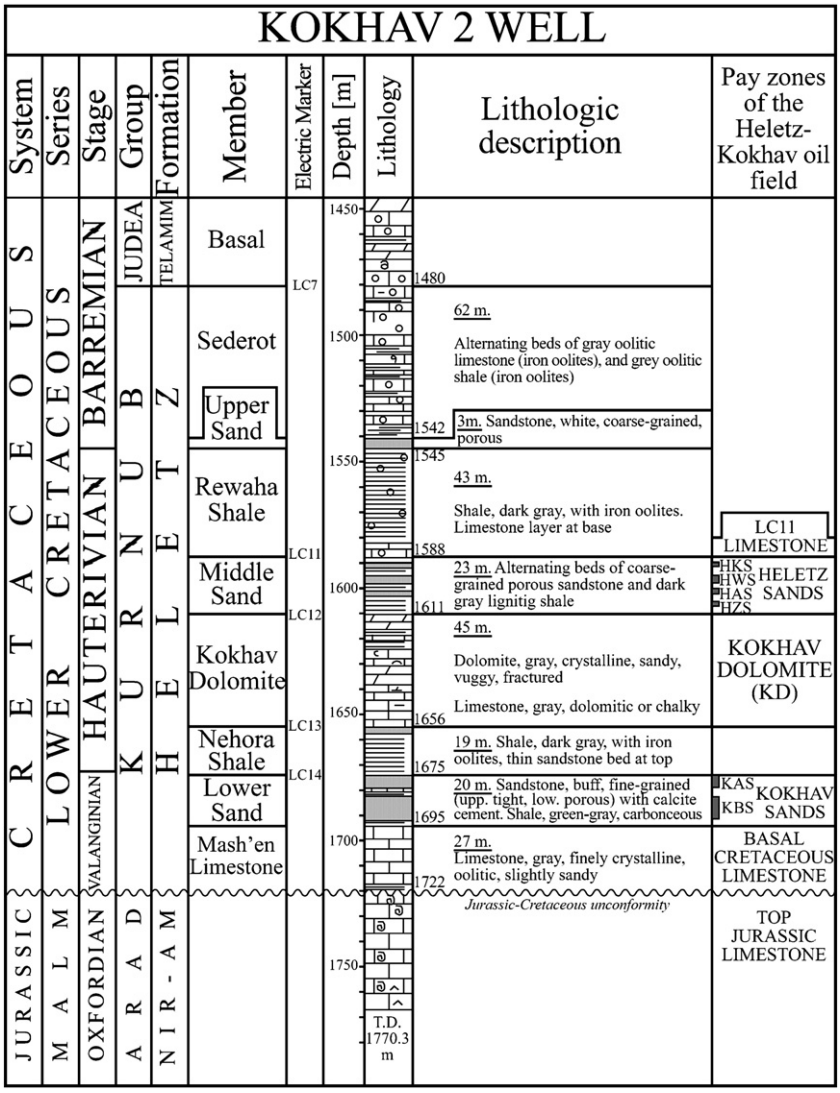

Fig. 3. Producing zones of the Heletz-Kokhav oil field, presented on the stratigraphic log of the Kokhav-2 borehole (modified after Shenhav, 1971).

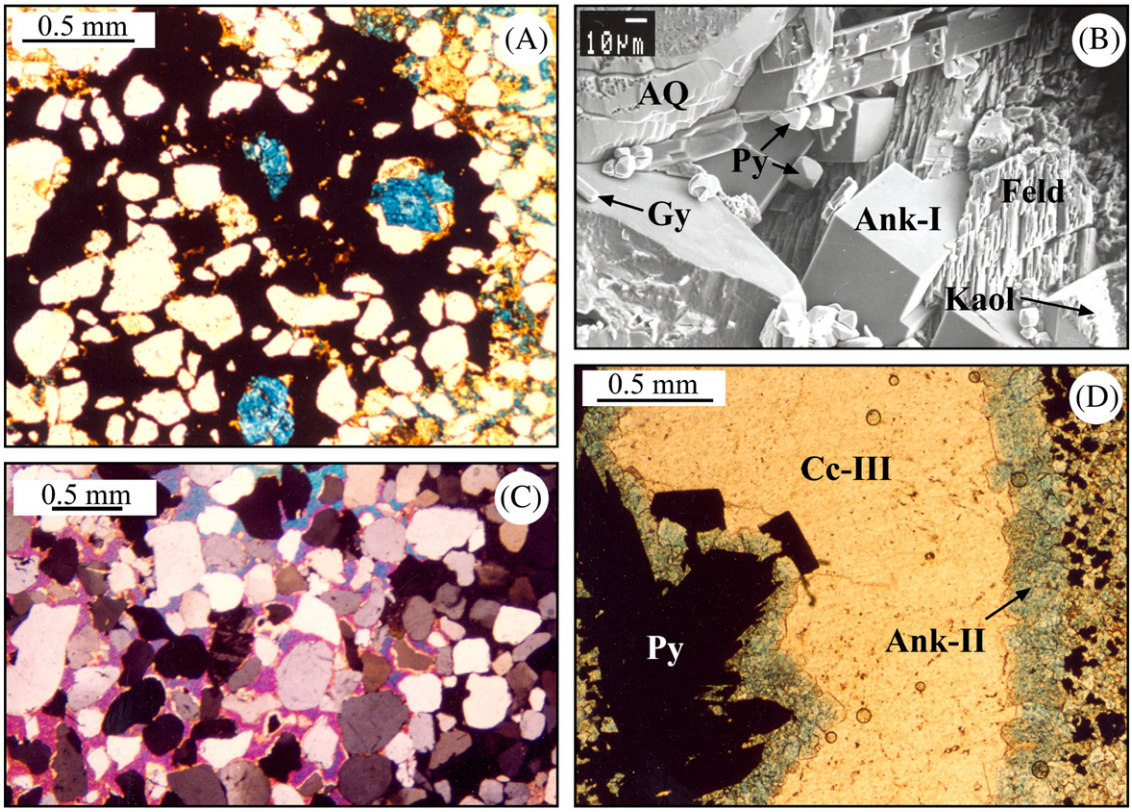

Fig. 4. (A) Fine-grain sandstone with hydrocarbons (black). The euhedral ankerite crystals (blue) replace detrital quartz grains (sample NR43, KS layer). (B) Detrital quartz and K-feldspar (Feld) grains in sandstone. The detrital quartz grain has an authigenic quartz overgrowth envelope (AQ). Ankerite (Ank-I phase), kaolinite (Kaol), pyrite (Py), and gypsum (Gy) fill pores (sample NR23, HKS layer). (C) Medium to fine-grain sandstone with poikilotopic calcite cement (Cc-II phase) (under cross polarized light; sample NR45, KS layer). (D) Massive pyrite (Py) pore-lining on walls of fractures in the Kokhav Dolomite Member. The pyrite was partly dissolved before the precipitation of the ankerite (Ank-II phase; blue). Sparry calcite (Cc-III phase) fills up and blocks the fractures (sample NR39, KD layer).

interpretation led Calvo et al. (1993) to suggest that the ankerite (deposited between ~90 and ~76 Ma ago; K-Ar ages of K-feldspar and illite, pre- and post-dating the ankerite formation, respectively) formed during the migration and accumulation of hydrocarbons in the Heletz reservoir; thus, accumulation of hydrocarbons in the Heletz trap started already during the Upper Cretaceous.

The $\delta^{18}O$ values of the present-day formation waters range from −2.19‰ to +5.33‰ (VSMOW) (Fleisher et al., 1977). Na/Cl and Cl/Br ratios of the formation water associated with the oil are close to those of seawater, with a total dissolved salt (TDS) of ~60 g/l (Starinsky, 1974). Starinsky's interpretation, that the waters in the formation (which are known as "Type C") are related to the Messinian (Upper Miocene) desiccation event of the Mediterranean Sea (Hsu, 1972), implies that the oils were probably generated and expelled from the source rocks and migrated into the Heletz Formation prior to that time.

3. Methods

Fifty-two core samples were selected from four boreholes in the Kokhav oil field (Kokhav 20, Kokhav 21, Kokhav 22, and Kokhav 23, Fig. 1), representing all of the reservoir intervals. These wells were chosen because they contain continuous cores of Heletz Formation rocks. The selected samples represent the variations in lithologies and textures within the different reservoir facies. Samples (rough and polished surface samples) were studied using a JEOL 840 scanning electron microscope (SEM) equipped with a LINK-10000 energy dispersive system (EDS). X-Ray diffraction (XRD), using a Philips PW 1820 with a Cu-Kα radiation (35 Kv and 35 mA) diffractometer, was employed to estimate the whole rock mineralogy, using form-factors calculated from synthetic mixtures of minerals on randomly oriented back-pack loaded samples. For stable isotopic analysis, organic matter was dissolved using 3% NaOCl for 12 h at room temperature. The samples were then washed several times with distilled water and oven-dried at 60 °C.

$\delta^{18}O$ and $\delta^{13}C$ analyses of the carbonate samples were made using a VG ISOCARB system attached to a SIRA-II Mass Spectrometer. The phosphoric acid extraction was carried out at 90 °C and the standards used for calibration were NBS-19 and an internal Carrara marble standard. All $\delta^{18}O$ and $\delta^{13}C$ values of the carbonate minerals are reported using the δ-notation relative to VPDB. $\delta^{18}O_{water}$ values are reported relative to VSMOW. The dolomite isotopic fractionation (α) was used in all calculations for ankerite. Using the ankerite values for α reported by Rosenbaum and Sheppard (1986) would have slightly lowered the values reported here, but would not have affected the discussion and conclusions that follow.

Carbonate mineral mixtures were prepared for isotopic analysis by reacting organic-free powdered rock samples in an off-line system (Single Vessel) in anhydrous H_3PO_4, following the procedures described by Walters et al. (1972) modified after McCrea (1950) and Epstein et al. (1964). The reaction times and temperatures for the different minerals were 2 h at 25 °C for calcite (Walters et al., 1972), 6 days at 25 °C for ankerite (Sullivan et al., 1990), and 1.5 h at 150 °C for siderite (Rosenbaum and Sheppard, 1986). Reproducibility (2σ) of the calcite internal standard was better than 0.1‰ for carbon and oxygen.

4. Results

4.1. Petrography and mineralogy

The petrography and paragenetic sequence of the Heletz Formation is discussed in detail by Calvo (1992). In summary, the

Table 1
General data of samples, mineralogy composition (XRD), ankerite chemistry, and carbonate stable isotope values.

Unit	Sample no.	Well name	Depth in well (m)	Elevation (relative to LC-12 marker) (m)	XRD composition[a]				EDS ankerite chemistry[b] (Ca,Mg,Fe,Mn) 2(CO3)3				Authigenic carbonate isotopic values[c]					
					Carbonate in whole rock	Ankerite	Calcite	Siderite	Ca	Mg	Fe	Mn	Ankerite		Calcite		Siderite	
													$\delta^{13}C$	$\delta^{18}O$		$\delta^{13}C$	$\delta^{18}O$	$\delta^{13}C$	$\delta^{18}O$
LC11	NR1	Kokhav 22	1599.4	24.5	56	39	61						−6.88	−2.56	Cc-I	1.15	−3.53		
	NR2	Kokhav 22	1600.1	23.8	77	55	45		1.2	0.61	0.19	0.01	−3.09	−2.15		−2.53	−3.46		
	NR5	Kokhav 22	1600.6	23.3	81	95		5					−1.43	−0.42					
	NR3	Kokhav 22	1602.1	21.8	65	100			1.12	0.58	0.28	0.01	−1.05	−1.73					
	NR4	Kokhav 22	1602.5	21.4	82	100			1.15	0.59	0.25	0.01	−3.73	−1.45					
	NR6	Kokhav 22	1603.1	20.8	20	100			1.11	0.56	0.32	0.01	−4.34	−4.27					
	NR23	Kokhav 21	1579.33	18.67	53	98		2	1.08	0.6	0.31	0.01	−4.03	−3.6				−4.22	1.45
HWS	NR25	Kokhav 21	1582.21	15.79	44	77		23	1.12	0.61	0.26	0.02	−5.24	−2.55				−2.65	−4.28
	NR26	Kokhav 21	1582.61	15.39	46	100			1.14	0.54	0.29	0.02	−6.59	−4.6					
	NR27	Kokhav 21	1582.75	15.25	37	100			1.01	0.65	0.32	0.02	−7.59	−4.43					
	NR7	Kokhav 22	1610	13.9	26	100			1.06	0.6	0.32	0.02	−7.73	−4.57					
	NR35	Kokhav 20	1550.32	13.78	32	100			1.03	0.65	0.3	0.02	−8.26	−4.5					
	NR9	Kokhav 22	1610.4	13.5	32	84	3	13					−8.81	−3.31					
	NR8	Kokhav 22	1610.9	13	13	100			1.03	0.62	0.33	0.02	−8.27	−4.32					
HAS	NR10	Kokhav 22	1613.5	10.4	36	100			1.08	0.58	0.32	0.02	−10.66	−4.03					
	NR28	Kokhav 21	1587.94	10.06	37	100			1.05	0.66	0.28	0.02	−9.04	−3.78					
	NR11	Kokhav 22	1614.3	9.6	97	100			1.07	0.63	0.28	0.02	−11.81	−4.13					
	NR12	Kokhav 22	1614.9	9	58	100			1.03	0.67	0.29	0.02	−11.92	−4.73					
	NR21	Kokhav 22	1615	8.9	32	100			1.06	0.54	0.38	0.02	−10.89	−3.77					
	NR13	Kokhav 22	1615.5	8.4	15	100			1.04	0.64	0.3	0.02	−11.66	−4.28					
	NR29	Kokhav 21	1590.65	7.35	15	100			1.11	0.52	0.36	0.01	−9.12	−3.07					
	NR14	Kokhav 22	1616.6	7.3	48	100			1.04	0.58	0.37	0.02	−11.09	−4.12					
	NR36	Kokhav 20	1557	7.1	34	100			1.08	0.56	0.34	0.01	−8.62	−3.61					
	NR22	Kokhav 22	1617.1	6.8	31	100			1.01	0.64	0.34	0.01	−9.86	−3.53					
	NR15	Kokhav 22	1618.1	5.8	23	87		13	1.09	0.62	0.28	0.02	−11.77	−3.52					
HZS	NR37	Kokhav 20	1561.22	2.88	49	27	63	10								−9.45	−6.02		
	NR30	Kokhav 21	1595.63	2.37	32	100							−7.04	−2.4					
	NR16	Kokhav 22	1622.2	1.7	16	94	6		1.16	0.54	0.28	0.02	−9.44	−3.34					
	NR38	Kokhav 20	1562.82	1.28	38	55	24	21	1.14	0.54	0.31	0.02	−6.57	−0.96		−5.33	−2.84		
KD	NR17	Kokhav 22	1625.3	−1.4	94	99	1		1.12	0.74	0.14	0.01	−3.36	−0.66					
	NR39	Kokhav 20	1566.39	−2.29	98	96	4						−5.21	−0.36					
	NR41	Kokhav 23	1640.08	−3.18	97	100			1.14	0.64	0.2	0.01	−4.35	0.15					
	NR31	Kokhav 21	1603.02	−5.02	97	29	71		1.17	0.67	0.16	0.01	−4.13	0.21		−1.6	−4.22		
	NR32	Kokhav 21	1604.28	−6.28	98	100			1.06	0.82	0.12	0	−1.6	−1.33					
	NR40	Kokhav 20	1571.57	−7.47	99	100			1.13	0.77	0.09	0.01	−1.79	0.52					
	NR33	Kokhav 21	1608.43	−10.43	98	100			1.09	0.72	0.18	0	0.04	−0.53					
	NR48	Kokhav 22	1634.7	−10.8	100		100									−5.27	−5.98		
KS	NR18	Kokhav 22	1695	−71.1	26	96	4		1.13	0.47	0.39	0.02	−3.35	−3.25					
	NR19	Kokhav 22	1695.8	−71.9	11	82		18	1.13	0.51	0.35	0.01	−2.06	−1.76					
	NR20	Kokhav 22	1696.4	−72.5	7	86		14	1.12	0.52	0.34	0.01	−9.87	−4.02					
	NR42	Kokhav 23	1712.87	−75.97	1	1	99									−8.05	−8.77		
	NR45	Kokhav 23	1714.86	−77.96	47		100									−1.77	−2.98		
	NR43	Kokhav 23	1715.04	−78.14	30	100			1.06	0.76	0.17	0.01	−3.68	−2.86					
	NR44	Kokhav 23	1716.36	−79.46	38	100			1.12	0.59	0.28	0.01	−5.01	−2.98					
Calcite veins in KD[d]	NR39-I	Kokhav 20	1566.39	−2.29	100		100								Cc-III	−5.19	−1.66		
	NR53-I	Kokhav 20	1566.9	−2.8	100		100									1.74	−2.32		
	NR52-I	Kokhav 21	1601.5	−3.5	100		100									−12.94	−6.58		
	NR50-I	Kokhav 22	1628.1	−4.2	100		100									−10.84	−6.65		
	NR51-I	Kokhav 21	1602.2	−4.2	100		100									−2.33	−5.72		
	NR49-I	Kokhav 22	1633.4	−9.5	100		100									−7.55	−5.39		
	NR49-II	Kokhav 22	1633.4	−9.5	100		100									−6.65	−5.61		
	NR47-I	Kokhav 22	1647.8	−23.9	100		100									−2.47	−6.44		
	NR47-II	Kokhav 22	1648.8	−23.9	100		100									−4.53	−6.86		

Remarks:
[a]Percents out of wholerock samples.
[b]Moles within ankerite formula.
[c]Isotopic data in permille units, relative to V-PDB standard.
[d]In very thick veins, two sample were taken, one near the contact (I), and one in the middle of the vein (II).

Heletz sands and Kokhav sands units (Middle Sand and Lower Sand members) are made up mainly of quartz-arenite to subarkose and arkose, and range from tuffaceous-sandstone to ankeritic-sandstone and siltstone. In places, mainly in pay-zone layers, hydrocarbons fill pores between grains (Fig. 4A). The Kokhav Dolomite Member consists mostly of ankeritic mudstone and biomicrite, with secondary porosity dominated by biomolds and fractures. The LC11 limestone layer is composed of ankeritic biosparite rich in iron-coated grains. Detrital components are mainly quartz and volcanic rock fragments. K-feldspar, plant and fauna remains, intraclasts, ooides, and heavy minerals are less frequent in the sandstones. Authigenic minerals in the Heletz Formation are dominated by carbonates (ankerite, calcite, and siderite), silicates (quartz, K-feldspar, kaolinite, illite, I/S, and smectite), and pyrite (Fig. 4B).

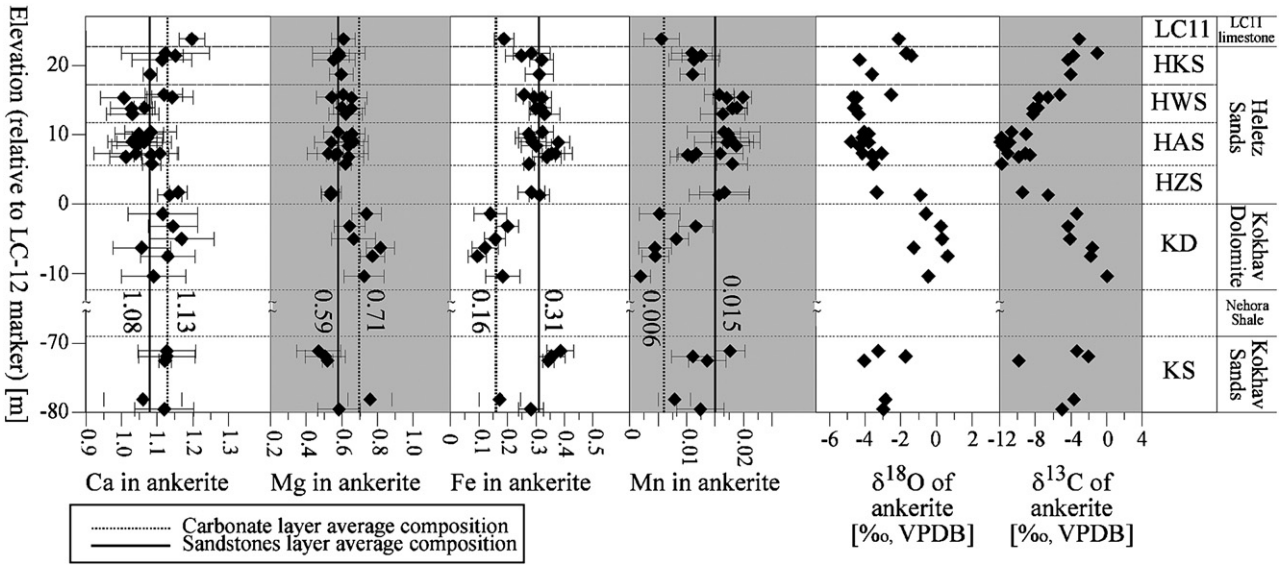

Fig. 5. Chemical composition (Ca, Mg, Fe, and Mn; mole number) and isotopic composition ($\delta^{18}O$ and $\delta^{13}C$) in ankerite cement in the Heletz Formation.

Calcite is the main cement mineral in the Kokhav sands unit (Lower Sand Member) (Fig. 4C). Fracture-related diagenesis of pyrite, ankerite, and calcite is found in veins and fractures in the dolostone rocks of the Kokhav Dolomite Member (Fig. 4D). The paragenetic sequence of cementation, dissolution and hydrocarbon emplacement is shown in Fig. 2.

4.2. Authigenic carbonate minerals

4.2.1. Ankerite and dolomite

Ankerite is the predominant authigenic cement mineral in the Heletz Formation (Table 1 and Fig. 2) and was formed during mesogenesis (Calvo, 1992; Calvo et al., 1993). It replaces calcite and dolomite precursors and detrital quartz grains and grows also as primary pore-filling euhedral rhombohedral crystals (Fig. 4A and B).

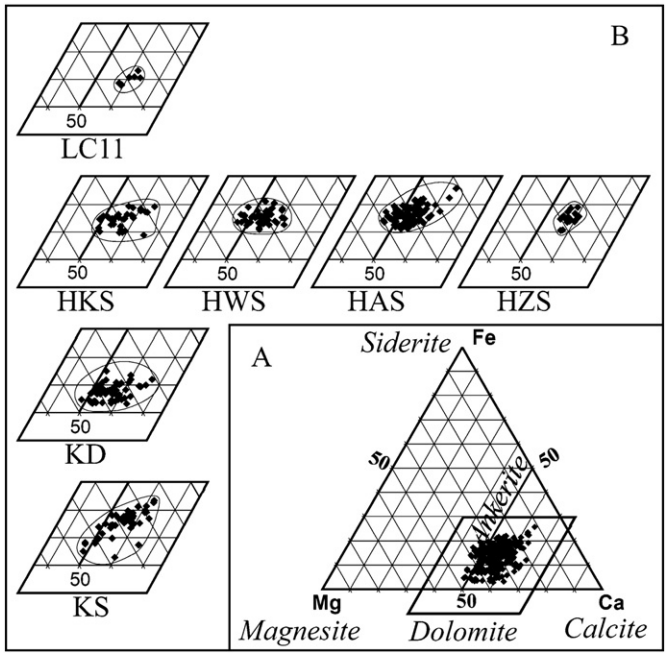

Fig. 6. Heletz Formation ankerite Ca-Mg-Fe triangle composition (A), and by members and pay-zone units (B), showing the lower Fe contents in the LC11 and KD carbonate units. The location of the frames in panel B is marked in panel A.

Previous work (Calvo, 1992; Calvo et al., 1993) indicates a calcic-ankerite composition [Ca>1 mole within $(Ca,Mg,Fe)_2(CO_3)_2$] in the Heletz Formation. More than 330 ankerite EDS analyses conducted in the current study on polished samples yielded an average composition of $Ca_{1.09}\ Mg_{0.62}Fe_{0.28}Mn_{0.013}(CO_3)_2$ for the ankerite in the Heletz Formation (Table 1 and Figs. 5 and 6). Ankerite cement from the clastic units (Heletz sands and Kokhav sands units; Middle Sand and Lower Sand members) has almost the same stoichiometric composition ($Ca_{1.08}\ Mg_{0.59}Fe_{0.31}\ Mn_{0.015}(CO_3)_2$), whereas the ankerite in the LC11 limestone layer and KD (Kokhav Dolomite) layer have higher Mg and Ca contents and significantly lower Fe and Mn ($Ca_{1.13}\ Mg_{0.71}Fe_{0.16}\ Mn_{0.006}(CO_3)_2$). The highest Fe content was measured in the HAS samples and the lowest Fe content characterizes the KD samples (Figs. 5 and 6).

The $\delta^{18}O$ values of the ankerite (40 samples) range from −4.73 to +0.52‰, and the $\delta^{13}C$ values range from −11.92 to +0.04‰ (Table 1, Figs. 5 and 7A). The ankerites in the sandstone layers usually have lower $\delta^{18}O$ and $\delta^{13}C$ values relative to those in the carbonate layers (Figs. 5 and 7A). The highest $\delta^{18}O$ and $\delta^{13}C$ values were measured in the Kokhav Dolomite Member (up to +0.52‰ and +0.04‰, respectively). The ankerite in the HAS sandstone layer has the lowest $\delta^{18}O$ and lowest $\delta^{13}C$ values (−4.73‰ and −11.92‰, respectively). In the HKS and HZS sandstone layers, the range of $\delta^{18}O$ variations is up to 3‰; with the highest isotopic values in samples that are closest to a carbonate layer (HKS toward the LC11 limestone layer, and HZS toward the Kokhav Dolomite layer) (Fig. 5).

Stoichiometric dolomite occurs in the Heletz Formation in small quantities and in two variations, the first variant, euhedral rhombohedra crystals floating in ankerite cement, and the second variation, as part of the vein filling carbonates in the Kokhav Dolomite rocks, along with some ankerite and calcite (Fig. 4D). Due to its scarcity in the formation (in both occurrences), chemical and isotopic analyses of dolomite were not performed in the current study.

4.2.2. Calcite

Calcite is less common than ankerite as cement in the Heletz Formation (Table 1). It occurs in three variations which were formed during different stages of diagenesis (Fig. 2): (1) eogenetic calcite replacing skeletal fragments in the LC11 limestone layer (referred to therein as Cc-I); (2) a later mesogenetic poikilotopic calcite cement in the Kokhav sands unit (Lower Sand Member) (Fig. 4C), co-genetic with the ankerite cementation (referred to as Cc-II); and (3) an

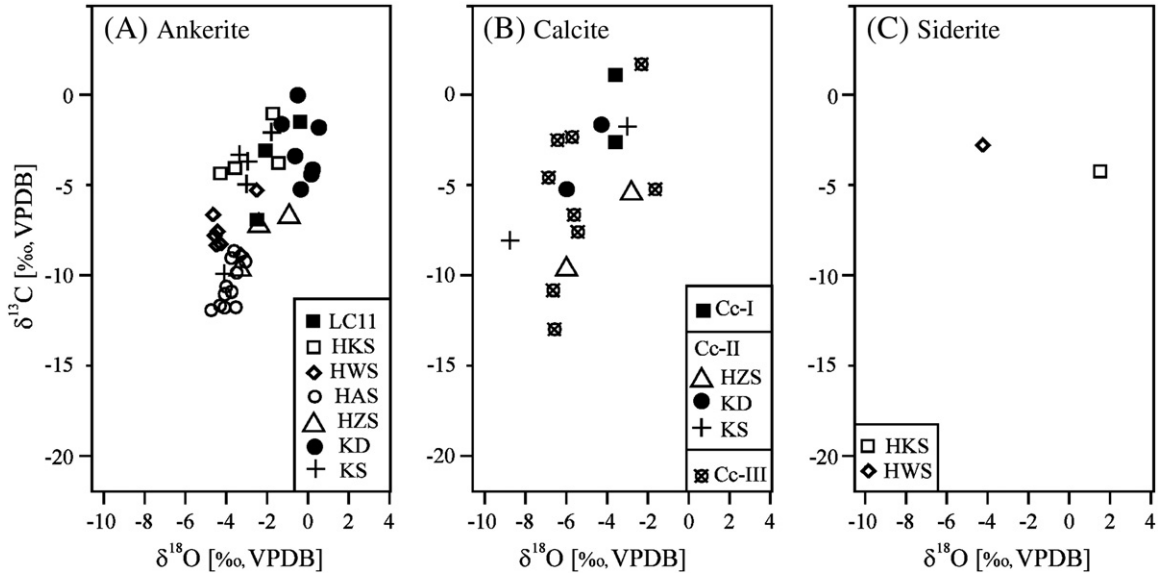

Fig. 7. $\delta^{13}C$ values plotted against $\delta^{18}O$ values of (A) ankerite, (B) calcite, and (C) siderite from the Heletz Formation. The $\delta^{13}C$ values of ankerite spread over a wide range of ~12‰ (−12 to 0‰), whereas those of $\delta^{18}O$ spread over a narrower range of ~5.2‰ (−4.7 to +0.5‰). Higher $\delta^{13}C$ and $\delta^{18}O$ values characterize the ankerite in the carbonate layers (LC11 limestone and Kokhav Dolomite Member), compared to the ankerite cement in the clastic units. The lowest $\delta^{13}C$ values characterize the ankerite cement from the HAS layer. $\delta^{13}C$ values of calcite spread over a very large range of about ~15‰ (−12.9 to +1.7‰) while $\delta^{18}O$ values are distributed over a narrower range of ~7.1‰ (−8.8 to −1.7‰).

epigenetic, fracture-related (Fig. 4D), vein-filling calcite in the Kokhav Dolomite Member (referred to as Cc-III).

EDS analyses of the Cc-II variety (total of 50 analyses) indicate a low-Mg calcite. The other two variations (Cc-I and Cc-III) were not analyzed in the current study. In a previous study (Calvo et al., 1993) it was found that the Cc-I variant is also a low-Mg calcite whereas the Cc-III variant is a high-Mg calcite.

Isotopic compositions of the three calcite variations are: Cc-I (2 samples) $-\delta^{18}O$ of −3.53 and −3.46‰, and $\delta^{13}C$ of −2.53 and +1.15‰; Cc-II (6 samples) $-\delta^{18}O$ of −8.77 to −2.84‰, and $\delta^{13}C$ of −9.45 to −1.60‰; and Cc-III (9 samples) $-\delta^{18}O$ of −6.86 to −1.66‰, and $\delta^{13}C$ of −12.94 to +1.74‰ (Table 1 and Fig. 7B).

4.2.3. Siderite

Siderite is a minor constituent in the Heletz Formation (Table 1). It occurs as euhedral to subhedral rhombohedra that formed early in the diagenetic history (Fig. 2).

Previous work (Calvo, 1992; Calvo et al., 1993) indicates a Ca-rich siderite with Fe>0.88 mol% and very low Mg/Ca ratios (close to zero).

The $\delta^{18}O$ values of the siderite ($n=2$) are −4.28 and +1.45‰, while the $\delta^{13}C$ values are −4.22 and −2.65‰ (Table 1 and Fig. 7C).

5. Discussion

Previous studies on the depositional environments of the Heletz Formation reported a marine and near-shore environment (Picard, 1959; Grader, 1959; Grader et al., 1960; Cohen, 1971), an epineritic environment (Boskovitz-Rohrlich, 1961), or a continental environment (Shenhav, 1971). Skeletal fragments (brachiopods, molluscs, algae, and echinoderms), that were recrystalyzed into calcite (Cc-I), indicate a contribution of near-shore environment products. Calvo (1992) and Calvo et al. (1993) suggested that the majority of the Heletz Formation section accumulated on-shore and incorporated, from time to time, fossil fragments from the near-shore environments. Chemical and isotopic data, combined with the paragenetic sequence, are used here to deduce changes in the pore-water chemistry and CO_2 sources during the diagenetic history of the Heletz Formation. Our approach was to construct a pathway of pore-fluid evolution that intersects the range of possible temperatures and $\delta^{18}O_{water}$ values for each diagenetic carbonate mineral in an order consistent with the paragenetic sequence and compatible with the geological history of the study area.

5.1. Eogenesis of calcite (Cc-I) and siderite

Calcite and siderite chemical and isotopic composition changes with the depositional environments (Mozley, 1989; Morad, 1998). In particular, the elemental and stable isotopic composition of early diagenetic siderite may be used to discriminate between marine and non-marine depositional environments (Mozley, 1989; Mozley and Wersin, 1992) and thus has potentially useful application in situations where depositional environment cannot be resolved by more traditional means (Baker et al., 1995). Marine siderites generally have lower $\delta^{13}C$ values than non-marine siderites, which themselves can have much lower $\delta^{18}O$ values than marine siderites (Mozley, 1989; Mozley and Wersin, 1992).

The calcite cement (Cc-I) in the Heletz Formation is a low-Mg calcite, typical of freshwater environments (Morad, 1998). The early diagenetic siderite cement in the Heletz Formation is a Ca-rich siderite with Fe>88 mol% and Mg/Ca~0, typical of meteoric regimes, where Fe>80 mol% and Mg/Ca << 1(Mozley, 1989). Both mineral compositions indicate a freshwater environment during the Heletz Formation early diagenesis. Using Mozley and Wersin (1992) discrimination, the siderite isotopic compositions could indicate that NR23 sample ($\delta^{18}O=+1.45$‰, $\delta^{13}C=-4.22$‰) was deposited in a more marine-orientated environment than NR25 sample ($\delta^{18}O=-4.28$‰, $\delta^{13}C=-2.65$‰).

Following the evidence that both minerals were formed early in the diagenetic history of the Heletz Formation, and most likely at a very shallow burial depth, the pore-water composition during their formation may indicate the environment of deposition for the Heletz Formation.

Using calcite-water oxygen isotope fractionation equations (O'Neil et al., 1969) for the calcite (Cc-I) values ($\delta^{18}O_{Cc\text{-}I}$ of −3.53 and −3.46‰) (Fig. 8A), and using early diagenetic temperatures (close to the surface or at shallow burial depth; 25–35 °C), the calculated formation pore-water isotopic values ($\delta^{18}O_{water}$) could range between −1.6 and +0.5‰ (Fig. 8B). Both calcite (Cc-I) samples could have formed from the same formation pore-water isotopic composition, with a slightly difference in formation temperature (Fig. 8B). This

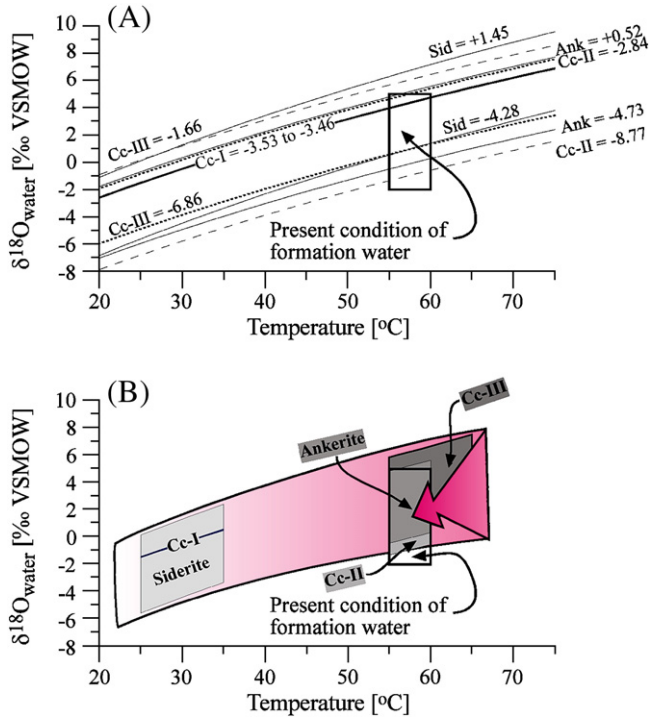

Fig. 8. (A) $\delta^{18}O$ values of formation water plotted against temperatures for diagenetic calcite, siderite, and ankerite from the Heletz Formation. The curves for these minerals are plotted for the maximum (top) and minimum (bottom) $\delta^{18}O$ values for each phase, using the following equations (T in °K in equations):1) $1000 \ln \alpha_{\text{calcite-water}} = 2.78*10^{-6}*T^{-2} - 2.89$ (O'Neil et al., 1969),2) $1000 \ln \alpha_{\text{ankerite-water}} = 2.78*10^{-6}*T^{-2} + 0.32$ (Dutton and Land, 1985),3) $1000 \ln \alpha_{\text{siderite-water}} = 3.13*10^{-6}*T^{-2} - 3.50$ (Rosenbaum and Sheppard, 1986). The present conditions are from Fleisher et al. (1977) and well logs. (55-60 °C and $\delta^{18}O_{\text{water}}$ of −3 to +5). (B) Suggested model for the pore-water evolution in the Heletz Formation, determined from the paragenetic sequence (Fig. 2) and the $\delta^{18}O$ values of the diagenetic minerals. Some of the relevant curves from panel A are also shown. Skeleton calcite (Cc-I) was formed early at, or close to surface conditions from brackish water ($\delta^{18}O_{\text{water}}$ −2 to 0). Siderite also formed early in the diagenetic history, but from more ^{18}O-depleted water ($\delta^{18}O_{\text{water}}$ −6 to +2). Calcite (Cc-II) and ankerite cements formed later at burial depth of ~1300 m (55 to 60 °C) from pore-water with $\delta^{18}O_{\text{water}}$ values of −0.5 to +5.5‰. The highest (+5.5‰) value indicates a long history of water–rock interaction prior to the ankerite deposition. Vein calcite (Cc-III) formed very late in the diagenetic history from water and temperatures which are very similar to the present-day conditions.

$\delta^{18}O_{\text{water}}$ range (−1.6 to +0.5‰), although based on only two samples, could indicate formation of the calcite (Cc-I) from a mixture of meteoric water with a brackish component, in good agreement with the chemical and mineralogical data, all indicate a freshwater dominated environment.

Using siderite-water oxygen isotope fractionation equations (Rosenbaum and Sheppard 1986) for the siderite values ($\delta^{18}O_{\text{Siderite}}$ of -4.28 and +1.45‰) (Fig. 8A), with the same temperature range (25−35 °C) will give a wider calculated $\delta^{18}O_{\text{water}}$ range (between −5.6 and +2.3‰) (Fig. 8B). Both siderite samples could not have formed from the same pore-water isotopic composition, even if using the full range of temperatures; the lowest $\delta^{18}O$ value for the heavier siderite sample at 25 °C (~ 0‰) is still heavier than the highest $\delta^{18}O$ value for the lightest siderite sample at 35 °C (~ −3.4‰) (Fig. 8B). These $\delta^{18}O_{\text{water}}$ values, although based on only two samples, indicate, at least for one of the samples, a much higher meteoric water component within the water mixture.

The $\delta^{13}C$ values of the calcite (Cc-I) (−2.53 and +1.15‰) are typical of a mixture of mainly inorganic atmospheric-derived CO_2 with small quantities from an organic CO_2 source, in good agreement with the purity of the calcite (low-Mg calcite) that implies formation within the oxic zone (Morad, 1998). The $\delta^{13}C$ values of the siderite (−4.22 and −2.65‰) are typical for a more organically derived CO_2 mixture, in good agreement with the occurrence of divalent Fe in the siderite, indicating a redox condition. The scarceness of siderite in the Heletz Formation (found only in 10 out of 45 samples, and maximum 10% (by mass) of siderite in the whole-rock) possibly indicates the rareness of the redox microenvironment conditions within a regional oxic environment during the early diagenesis stage.

In summary, based on the petrography, mineralogy, chemical composition and isotopic data of early diagenetic calcite and siderite, the Heletz Formation was deposited in a terrestrial environment of a mainly freshwater composition, with low quantities of organic matter.

5.2. Mesogenesis of ankerite and calcite (Cc-II)

During the rapid Middle Cretaceous burial, silicate minerals were formed (quartz and K-feldspar overgrowths) and carbonate minerals were partly dissolved (Calvo, 1992; Calvo et al., 1995). Ankerite formation followed the authigenic K-feldspar and pre-dated the illite formation (Fig 2). The K-Ar ages of the authigenic K-feldspar were dated to ~90 Ma, and that of the illite was dated to ~76 Ma (Calvo, 1992; Calvo et al., 1995). Petrographic relationship between hydrocarbon and ankerite cement (Fig. 4A) was interpreted as if the hydrocarbon accumulation within the Heletz Formation stratigraphic and structural trap started at the same stage as the ankerite precipitation (Calvo, 1992; Calvo et al., 1995). Based on the back-stripping burial profile (Fig. 9), a burial depth of 1200 to 1400 m was calculated for that stage. Assuming a constant temperature gradient of 25 °C/km (Levy, 1981), this depth corresponds to burial temperatures of 55 to 60 °C. The petrographic evidence indicates that the low-Mg calcite (Cc-II) poikilotopic calcite cement in the sandstone units (Fig. 4C) grew simultaneously with the ankerite; that is, at the same burial depth.

The observed isotopic values ($\delta^{18}O_{\text{Ankerite}}$ −4.73 to +0.52‰, $\delta^{18}O_{\text{Cc-II}}$ −8.77 to −2.84‰) (Fig. 8A) and the assumed temperature range of 55 to 60 °C during precipitation of ankerite and calcite (Cc-II) are related to the pore-water composition through the fractionation equation of ankerite (Dutton and Land, 1985) and of calcite (O'Neil et al., 1969). The calculated $\delta^{18}O_{\text{water}}$ values for both minerals are quite similar, ranging from −1.4 to +6.4‰ for calcite (Cc-II) and from −0.5 to +5.5‰ for ankerite (Fig. 8B), indicating that the pore-water in the Heletz Formation became more ^{18}O-enriched during burial. This is typical of most sedimentary basins as rock–water interaction associated with dissolution of marine carbonates and silicates leads to ^{18}O-enriched water (Longstaffe, 2000).

The low $\delta^{13}C$ values of calcite (Cc-II) (−9.45 to −1.60‰) and that of ankerite (-11.92 to +0.04‰), much lower than those measured for calcite (Cc-I) and siderite, formed in the eogenesis stage, indicate the dominance of organic-derived CO_2. Decomposition of organic matter forms isotopically light CO_2 with $\delta^{13}C$ as low as −25‰ (e.g., Irwin et al., 1977; Matsumoto and Iijima, 1981; Dutton and Land, 1985; Sullivan et al., 1990).

EDS measurements of most of the ankerite in the Heletz sands unit (Middle Sand Member) (HKS, HWS, HAS, and HZS) indicate a rather homogenous composition, with a stoichiometric average of $Ca_{1.08}Mg_{0.60}Fe_{0.31}Mn_{0.015}(CO_3)_2$ (Fig. 6B).

The Fe in the ankerite lattice displays a negative correlation with Mg ($R = -0.82$), and a positive one with Mn ($R = +0.69$) (Table 2), in agreement with the observations of Gawthorpe (1987) on many other ankerites. Mg in the ankerite lattice is correlative best with Fe ($R = -0.82$), less significant with Mn (R = -0.53), and very poorly with Ca ($R = -0.30$). The increase in carbonate alkalinity in the suboxic zone enhances the precipitation of carbonate cement with a slight enrichment in Mn and Fe coupled with depleted $\delta^{13}C$ (Morad et al., 1998).

Both Fe and Mn in the ankerite lattice display a significant negative correlation with $\delta^{13}C$ values (R = -0.69 and -0.73, respectively; Fig. 10 and Table 2), attesting to the control of redox microenvironments established due to the organically derived CO_2 in the pore-water.

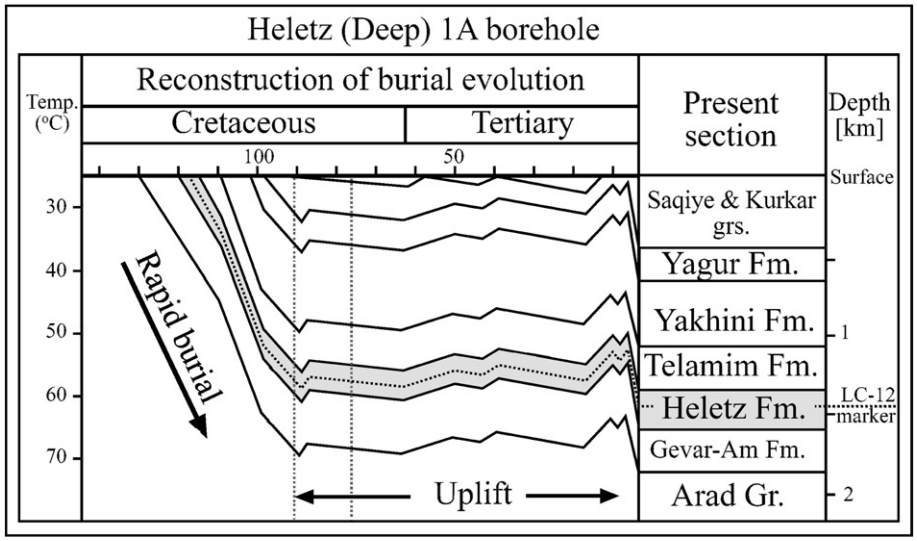

Fig. 9. Backstripping burial curve for the Heletz 1A Deep borehole (after Feinstein, S., personal communication) emphasizing the rapid burial rate (~50 m/Ma) during the Cretaceous, the Syrian Arc Fold uplift (Upper Cretaceous), and the Miocene uplift. The Heletz Formation was deposited during the Lower Cretaceous and was buried to its maximal depth already in the Upper Cretaceous. Dashed lines (~90 Ma and ~76 Ma) are for the K-Ar ages of two authigenic K-bearing minerals (K-feldspar and illite); at this age the ankerite and calcite (Cc-II) were formed and the hydrocarbons started to accumulate.

A significant correlation is observed in the Heletz Formation ankerite between the stratigraphic location of the layers and the $\delta^{13}C$ values; the $\delta^{13}C$ values decrease significantly as the HAS sandstone layer is approached from above and from below it (Fig. 5). Since $\delta^{13}C$ is negatively correlated with Fe and with Mn (Table 2), an opposite trend is also observed between the stratigraphic location, on the one hand, and Fe and Mn values, on the other hand (Fig. 5).

The single factor that links these observations and trends seems to be related to the source of the organic matter and the redox potential. This is ascribed to the HAS sandstone layer, which is the main producing pay-zone unit in the Heletz Formation (Gilboa et al., 1990), and to the petrographic evidence of the timing of ankeritization in Late Cretaceous during hydrocarbon migration.

During the Upper Cretaceous, in addition to the carbonate minerals, authigenic silicate minerals (mainly kaolinite and illitic clays) also formed. At that time, the tectonic activity of the Syrian Arc fold system had already formed the anticlinal structure of the Heletz trap (Gilboa et al., 1990).

5.3. Epigenetic, fracture-related vein filling of ankerite, dolomite, and calcite (Cc-III)

Fracture-related carbonate diagenesis was observed in the KD unit. The paragenetic sequence within the veins started with ankerite, followed by dolomite and terminated with calcite (Cc-III) (Fig. 4D). Based on the petrographic and mineralogical constrains, it is suggested that calcite (Cc-III) was formed from brackish water that penetrated into the subsurface during the Messinian desiccation event (Fig. 2).

Table 2
Correlation coefficients (*R*) for ankerite cement chemistry in the Helatz Formation.

	Mg	Fe	Mn	d18O	d13C
Ca	−0.3	−0.3	−0.32	0.57	0.49
Mg		−0.82	−0.53	0.38	0.29
Fe			0.69	−0.71	−0.69
Mn				−0.73	−0.73
$\delta^{18}O$					0.71

Based on the geological history of the Heletz area, sediment unloading and fracturing probably occurred during the Miocene Messinian Mediterranean Sea aridity (some 6 Ma ago), leading to erosion of the overburden section above the Heletz Formation (Fig. 9). The Messinian brine infiltrated the permeable carbonate rocks of the Judea group which were exposed along the coast, and the brines subsequently migrated down into the sandy Heletz Formation and came into direct contact with the oil therein (Chan et al., 2002).

The burial depth was still very close to that of the former diagenetic stage, but the mixing of the formation water with evaporated seawater penetrating the subsurface of the Israeli coastal plain (Starinsky, 1974) significantly changed the chemical and isotopic composition of the pore-water.

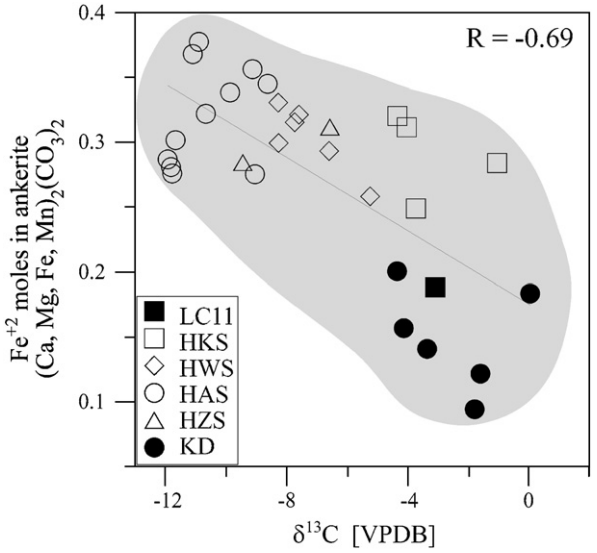

Fig. 10. $\delta^{13}C$ values plotted against moles of $FeCO_3$ in the lattice of Heletz Formation ankerites. The significant negative correlation between the Fe content and the organically derived CO_2 (expressed in low $\delta^{13}C$ values) indicates that the reducing conditions were caused by the decomposition of organic matter, most likely hydrocarbons.

Using the $\delta^{18}O_{Cc\text{-}III}$ values of the high-Mg calcite (Cc-III) (−6.86 to −1.66‰) and a temperature range of 55–60 °C in the calcite-water fractionation equation (O'Neil et al., 1969), yields calculated $\delta^{18}O_{water}$ values in the range of +0.6 to +7.3‰ (Fig. 8). Without taking into consideration the fracture-related occurrence of the Cc-III calcite, its chemical composition (high-Mg calcite) could have been explained by its stratigraphic location within Kokhav Dolomite unit, and its (ca.) pore-water composition ($\delta^{18}O_{water} = +1$ to +7‰) as reflecting a very extensive water–rock interaction within the Heletz Formation. Since it is part of a vein-filling carbonate mineral sequence (ankerite-dolomite-calcite; Fig. 4D) located within fractures, we prefer to explain this sequence and the calcite (Cc-III) chemical and isotopic values to be derived by the chemical and isotopic signature of the evaporated sea-water, penetrating the Heletz Formation during the Messinian event (Starinsky, 1974).

The $\delta^{13}C$ values of calcite (Cc-III) (−12.94 to +1.74‰), which are similar to the mesogenetic ankerite (~ −12‰ to ~0‰), also indicate the dominance of organic-derived CO_2.

6. Summary and conclusions

In the current study we explored the pore-water evolution during burial and diagenesis, based on the chemical and isotopic signatures of the carbonate cement mineral in the Heletz Formation.

Early in the diagenetic history (some ~125 Ma ago), skeletal material was recrystallized and filled with low-Mg calcite (Cc-I). Calcic-siderite was also formed at this stage, mainly in clastic units. Stable isotope data indicate that these minerals formed from meteoric water, which were in places oxic or reducing.

Later in the diagenetic history (between 90 and 76 Ma ago) dolomite, ankerite and calcite (Cc-II) cements formed. The morphology of the ankerite indicates that it is mostly primary (precipitated directly from water). Ankerites from the different clastic units have almost the same stoichiometric composition, whereas the ankerites in the carbonate layers have higher Mg and Ca contents and significantly lower Fe and Mn, indicating that as opposed to the clastic units, where ankerite growth was mostly primary, in the carbonate layers, ankerite replaced calcite and dolomite precursors. The $\delta^{13}C$ values of calcite (Cc-II) and of ankerite phases (as low as -13‰) indicate a significant contribution of organic-derived CO_2, in good agreement with the petrographic observation that hydrocarbon accumulation and ankerite precipitation were contemporaneous.

About ~6 Ma ago, fractures in the Kokhav Dolomite Member were filled with ankerite, dolomite, and calcite (Cc-III). The chemical composition of the calcite (Cc-III) phase indicates a mixture with marine-derived waters. While the $\delta^{18}O$ values are not conclusive (do not show large differences from previous carbonate phases), the $\delta^{13}C$ values clearly indicate a mixture of the formation waters with marine-derived water.

Based on the $\delta^{18}O$ values of the carbonate minerals, mineral–water fractionation equations, burial depths and temperature estimate, we could calculate the oxygen isotopic composition of the formation water and chemical variations with time. Early in the diagenetic history the water composition was mainly meteoric (as low as −5.6‰), but during burial history, water–rock interactions led to much higher $\delta^{18}O$ values of the pore water (as high as +6.4‰).

The $\delta^{13}C$ values of the carbonate minerals serve as a very good proxy for the CO_2 source. Early in the diagenesis, the main source for CO_2 was atmospheric, together with ^{13}C-depleted soil-CO_2 but later, during hydrocarbon accumulation, the CO_2 source was mainly organic (as low as -13‰) and finally, during the Messinian seawater invasion, seawater CO_2 was mixed with the organic CO_2 pool.

To conclude, the results of the present study indicate that oil migrated into the Heletz formation already during the Upper Cretaceous and strongly controls the diagenetic phase sequence and their isotopic composition.

Acknowledgments

We wish to acknowledge the Geological Survey of Israel for their financial and technical support. Thanks are due to Mrs. Beverly Katz and the anonymous reviewers for their highly constructive review of this manuscript.

References

Aharoni, E., 1964. Litho-electric correlation of the Kurnub Group (Lower Cretaceous) in the Northern Negev. Israel Journal of Earth Sciences 13, 63–81.
Baker, J.C., Kassan, J., Hamilton, P.J., 1995. Early diagenetic siderite as an indicator of depositional environment in the Triassic Rewan Group, southern Bowen Basin, eastern Australia. Sedimentology 43, 77–88.
Bein, A., Gvirtzman, G., 1977. A Mesozoic fossil edge of the Arabian Plate along the Levant coastline and its bearing on the evolution of the Eastern Mediterranean. In: Biju-Duval, B., Montadert, L. (Eds.), Structural History of the Mediterranean Basin, pp. 95–110.
Bein, A., Sofer, Z., 1987. Origin of oils in Heletz region, Israel — implications for exploration in the Eastern Mediterranean. American Association of Petroleum Geologists Bulletin 71, 65–75.
Boskovitz-Rohrlich, V., 1961. Oolitic iron ores of Lower Cretaceous age in Israel and the problem of their origin. Ph.D. thesis, The Hebrew University of Jerusalem, 101 p. (in Hebrew, with English abstract).
Calvo, R., 1992. The diagenetic history of Heletz Formation and the timing of hydrocarbons accumulation in Heletz-Kokhav oil field. M.Sc. thesis, The Hebrew University of Jerusalem, 72 p. (in Hebrew, with English abstract).
Calvo, R., Ayalon, A., Bein, A., Sass, E., 1993. Diagenetic history of the Heletz Formation and the timing of hydrocarbon accumulation in the Heletz-Kokhav oil field. Geological Survey of Israel, Current Research 8, 82–83.
Calvo, R., Bein, A., Sass, E., Ayalon, A., 1995. The diagenetic history of the Heletz Formation and the timing of hydrocarbon accumulation in Heletz-Kokhav Oil Field. Geology of the Eastern Mediterranean Region, 2nd International Symposium, p. 3.
Chan, L.-H., Starinsky, A., Katz, A., 2002. The behavior of lithium and its isotopes in oilfield brines: evidence from the Heletz–Kokhav field, Israel. Geochimica et Cosmochimica Acta 66, 615–623.
Cohen, Z., 1971. The geology of the Lower Cretaceous in Southern Coastal Plain. Ph.D. thesis, The Hebrew University of Jerusalem, 98 p. (in Hebrew, with English abstract).
Dutton, S.P., Land, L.S., 1985. Meteoric burial diagenesis of Pennsylvanian arkosic sandstones, Southwestern Anadarko Basin, Texas. American Association of Petroleum Geologists Bulletin 69, 22–38.
Epstein, S., Graf, D.L., Degens, E.T., 1964. Oxygen isotope son the origin of dolomite. In: Craig, H., Miller, S.L., Urey, H.C., Wasserburg, G.J. (Eds.), Isotopic and Cosmic Chemistry. North Holland Publishing Company, Amsterdam, pp. 169–180.
Fleisher, E., Goldberg, M., Gat, J.R., Magaritz, M., 1977. Isotopic composition of formation waters from deep drillings in southern Israel. Geochimica et Cosmochimica Acta 41, 511–525.
Gawthorpe, R., 1987. Burial dolomitization and porosity development in a mixed carbonate-clastic sequence: an example from the Bowland Basin, northern England. Sedimentology 34, 533–558.
Gilboa, Y., Fligelman, H., Derin, B., 1990. Heletz-Brur-Kokhav Field - Israel southern Coastal Plain. In: Beaumont, E.A., Foster, N.H. (Eds.), Treatise of Petroleum Geology, Atlas of Oil and Gas Fields Structural Trap IV - Tectonic and Non Tectonic Fold Trap, pp. 319–395.
Grader, P., 1959. The geology of the Heletz oil field. Ph.D. thesis, The Hebrew University of Jerusalem, 81 p. (in Hebrew, with English abstract).
Grader, P., Reiss, Z., Klug, K., 1960. Correlation of subsurface Lower Cretaceous units in the southern coastal plain of Israel. Geological Survey of Israel, Bulletin No. 28 7 p.
Hsu, K.J., 1972. When the Mediterranean dried up. Scientific American 227, 27–36.
Irwin, H., Curtis, C., Coleman, M., 1977. Isotopic evidence for source of diagenetic carbonates formed during burial of organic-rich sediments. Nature 269, 209–213.
Levy, Y., 1981. Determination of degree of coalification by UV-fluorescence of spores and vitrinite reflectance from Triassic, Jurassic and Lower Cretaceous rocks of the northern Negev and southern Coastal Plain of Israel. M.Sc. thesis, Ben Gurion University, 116 p. (in Hebrew, with English abstract).
Longstaffe, F.J., 2000. An introduction to stable oxygen and hydrogen isotopes and their use as fluid tracers in sedimentary systems. In: Kyser, T.K. (Ed.), Fluids and Basin Evolution. Mineralogical Association of Canada, Short Courses, pp. 115–163. 28.
Matsumoto, R., Iijima, A., 1981. Origin and diagenetic evolution of Ca-Mg-Fe carbonates in some coalfields of Japan. Sedimentology 28, 239–259.
McCrea, J.M., 1950. On the isotopic chemistry of carbonates and a paleotemperature scale. The Journal of Chemical Physics 18, 849–857.
Morad, S., 1998. Carbonate cementation in sandstones: distribution patterns and geochemical evolution. Special Publication International Association of Sedimentologists, Carbonate Cementation in Sandstone 26, 1–26.
Morad, S., Ben Ismail, H.N., De Ros, L.F., Al-Aasm, I.S., Serrhin, N.-E., 1994. Diagenesis and formation water chemistry of Triassic reservoir sandstones from southern Tunisia. Sedimentology 41, 1253–1272.
Morad, S., De Ros, L.F., Nystuen, J.P., Bergan, M., 1998. Carbonate diagenesis and porosity evolution in sheet-flood sandstones: evidence from the Middle and Lower Lunde members (Triassic) in the Snorre Field, Norwegian North Sea. Special Publication

International Association of Sedimentologists, Carbonate Cementation in Sandstone 26, 53–85.
Mozley, P.S., 1989. Relation between depositional environment and the elemental composition of early diagenetic siderite. Geology 17, 704–706.
Mozley, P.S., Wersin, P., 1992. Isotopic composition of siderite as an indicator of depositional environment. Geology 20, 817–820.
O'Neil, J.R., Clayton, R.N., Mayeda, T.K., 1969. Oxygen isotope fractionation in divalent metal carbonate. The Journal of Chemical Physics 51, 5547–5558.
Picard, L., 1959. Geology and oil exploration in Israel. Bulletin of Research Council of Israel, Section G: Geo-Science 8, 1–30.
Rosenbaum, J., Sheppard, S.M.F., 1986. An isotopic study of siderites, dolomites and ankerites at high temperatures. Geochimica et Cosmochimica Acta 50, 1147–1150.
Shenhav, H., 1971. Lower Cretaceous sandstone reservoirs, Israel: petrography, porosity, permeability. American Association of Petroleum Geologists Bulletin 55, 2194–2224.
Starinsky, A., 1974. Relationship between Ca-chloride brines and sedimentary rocks in Israel. Ph.D. thesis, The Hebrew University of Jerusalem, 84 p. (in Hebrew, with English abstract).
Sullivan, M.D., Haszeldine, R.S., Falick, A.E., 1990. Linear coupling of carbon and strontium isotopes in Rotliegend Sandstone, North Sea: evidence for cross-formational fluid flow. Geology 18, 1215–1218.
Walters Jr., L.J., Claypool, G.E., Choquette, P.W., 1972. Reaction rates and ^{18}O variations for the carbonate-phosphoric acid preparation method. Geochimica et Cosmochimica Acta 36, 129–140.